CCN/IFN AND THE ARCTIC SURFACE ENERGY BUDGET

Gustavo Carrió, H. Jiang and W. R. Cotton
Colorado State University, Fort Collins, Colorado

1. INTRODUCTION

The potential impact of intrusions of polluted air into the Arctic basin on sea-ice melting/freezing rates and the surface energy budget is examined. Previous studies (Carrió et al., 2003a and b) focused on the impact of IFN entrainment from above the inversion on sea-ice melting rates for the spring period. The present paper examines the impact of enhancing both IFN and CCN concentrations above the boundary layer, and extends the cloud-resolving simulations (CRM) to a 9-month period covering the fall, winter and spring seasons during the 1997-1998 SHEBA field campaign. We implemented the Los Alamos National Laboratory sea-ice model (CICE) into the research and real-time versions of the Regional Atmospheric Modeling System at Colorado State University (RAMS@CSU). Aerosol profiles based on May 4 1998 observations were used to characterize the polluted upper layer. The 2-3 daily SHEBA soundings were utilized to provide time-evolving boundary conditions. Results indicate that the IFN entrainment from above the inversion decreases the freezing rates and increases the melting rates when mixed-phase clouds are present. An opposite, although less important effect can be associated with CCN entrainment when liquid-phase clouds prevail.

2. MODEL DESCRIPTION

The model used in this study is the cloud resolving version of RAMS@CSU (Cotton et al., 2003). The new microphysical package (Saleeby and Cotton, 2003) shares the double moment microphysical framework of the previous scheme assuming that hydrometeor size spectra have a gamma distribution function and mass mixing ratio as well as number concentration of the hydrometeor species is predicted. However, among other new features it explicitly considers the nucleation of cloud droplets via activation of CCN, and a bimodal representation of spectrum of liquid particles. The predicted microphysical categories also include the number concentration and mixing ratio of rain, pristine ice, snow, aggregates, graupel and hail, as well as the IFN and CCN concentration. The original version of CICE (Hunke and Lipscomb, 1999) was modified in its structure to allow module communication in an interactive multi-grid framework. This sea-ice model discretizes the sub-grid ice thickness distributions in different categories, considering their corresponding fractional areas as prognostic variables.

Corresponding author's address : Gustavo G. Carrió, Atmospheric Science Department, Atmospheric Science Bldg., Colorado State University, Fort Collins CO 80523, USA; e-mail: carrio@atmos.colostate.edu

Ice thickness categories are partitioned in a number of internal ice layers. For each thickness category, the surface and snow temperatures as well as the temperatures associated with the internal layer are also prognostic variables.

3. EXPERIMENT DESIGN

Fall-winter simulations were initialized on Oct 16 1997 with a simulation time of 195 days (Oct16-May 1), while spring-summer numerical experiments covered the a 92-day period (May 1-July 31). All these experiments have been performed in a two-dimensional (2-D) framework. Model domain was 5000m in the horizontal and approximately 3325m in the vertical. A constant horizontal resolution of 50m, a vertical resolution of 30m, and a timestep of 2s were used. The lateral boundary conditions were cyclic and the domain top is a rigid lid.

Observed aerosol profiles (May 4 1998) were used as a benchmark although IFN and CCN concentrations were assumed to be constant with altitude within the upper layer (at time=0). The simulations were initialized using different IFN and CCN profiles based on those observed *above the inversion*. Conversely, *within the boundary layer* the initialization profiles for all experiments assume "clean" concentrations of IFN and CCN (3 L^{-1}, 100cm^{-3}, respectively). Only the initialization profiles corresponding to the control run assume "clean" IFN profiles for both layers. In order to isolate the effect of the entrained aerosols efficiently, a Newtonian relaxation technique (nudging) was applied to restore the polluted and clean aerosol concentrations above and below the current altitude of the inversion, respectively. For this reason, the initialization profiles associated with the observations (hereafter referred to as "observed") were defined as a vertical average of the observed aerosol profiles within the upper layer, instead of retaining their vertical structure as done by Carrió et al. (2003a)

For both sensitivity tests, six ice thickness categories (with 4 internal layers) are considered to describe the sub-grid ice thickness distribution. The mass and energy-conserving remapping scheme of Lipscomb (2001) is used to transfer ice among categories. The SHEBA daily time series of divergence and shear rates were used to take into account the changes in thickness distribution associated with ice dynamics. Ice thickness was initialized with values of 1.5 and 2.41m for the fall-winter and spring-summer numerical experiments, respectively.

A summary of multi-month CRM simulations we performed is given in Table 1. All, these runs have been performed for both simulation periods. Additionally, some numerical experiments have been initialized in October 16 1997 but also run for the entire simulation period (Oct 16-Jul 31).

Table I

EXP	IFN	CCN
1*	clean	Clean
2	clean	100% obs
3*	50% obs	Clean
4*	50% obs	100% obs
5	75% obs	100% obs
6*	100% obs	Clean
7	75% obs	75% obs
8*	100% obs	100% obs
9	125% obs	125% obs

* denotes the numerical experiments that have also been run for the entire simulation period.

4. RESULTS

We generated probability density functions (PDFs) of some microphysical variables associated with ice-phase particles for the entire 9-month period. Figure 1 gives the PDFs of total ice number concentration (Ni) and mean mass diameter (Di) of precipitating ice particles. Increasing IFN within the upper layer reduces the mode of Di and increases the frequency of large values of Ni.

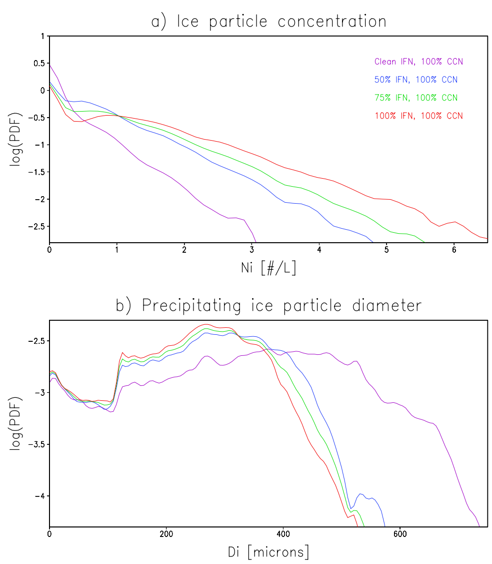

Figure 1. PDF's for Ni (a) and Di (b) .

Substantial differences can also be observed between runs that consider enhanced IFN concentrations in PDFs of ice water path (IWP), total condensate path (TCP), and longwave down (LWDN) (not shown). The larger values of these quantities exhibit a monotonic behavior increasing their frequency when a more polluted upper layer is assumed.

The simulated longwave downwelling radiative flux at the surface (LWDN) is compared for the control run and the run that nudges the observed profiles in Fig. 2a. These LWDN differences of with respect to the control run have been computed using hourly horizontal averages. Positive differences prevail indicating an increase of LWDN due to the aerosol entrainment. A Scatter plot of LWDN differences against those corresponding to TCP is given in Fig. 2b This scatter plot reveals an important degree of association between the changes in LWDN and TCP differences induced by aerosol entrainment. Similar numerical experiments have been performed for a CCN concentration 50% higher, although the main results of Figs. 2 remained unaltered.

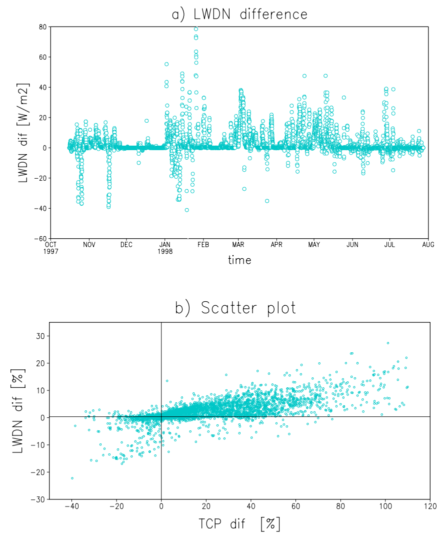

Figure 2. LWDN difference (a). Scatter plot for LWDN and TCP percent differences (b).

Figures 3. and 4. are analogous to Fig. 2 but for the shortwave downwelling radiative flux at the surface (SWDN), and for the net radiative forcing (NETRAD).

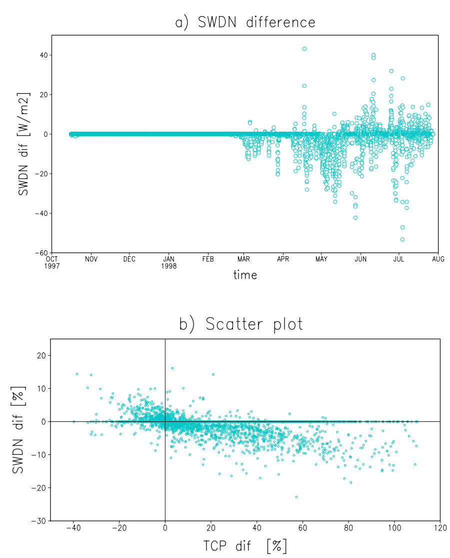

Figure 3. SWDN difference (a). Scatter plot for SWDN and TCP percent differences (b).

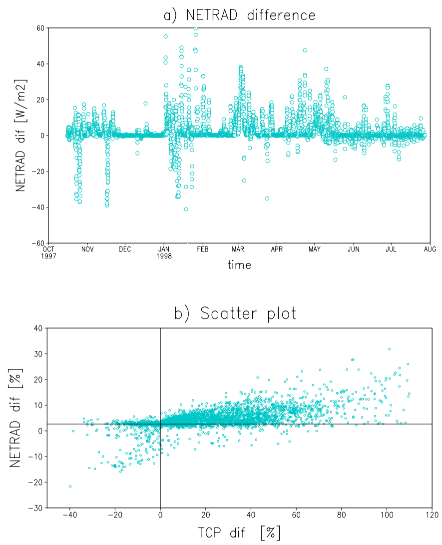

Figure 4. NETRAD difference (a). Scatter plot for NETRAD and TCP percent differences (b).

When we compare SWDN, negative differences with respect to the control are more frequent, while positive differences prevail for NETRAD. A significant degree of association can be seen between the change in these fluxes and the percent difference in TCP. The magnitude of the differences in LWDN, SWDN, and NETRAD vary in a monotonic manner when nudged IFN concentration increase from clean to 50, 75 and 100% of the observed (not shown).

Differences of the simulated sea-ice thickness with respect to the control run are plotted in Fig. 5a. The cloud liquid fraction, evaluated as the ratio between the liquid water path and TCP of all vertical columns of the domain is given in Fig 5b for the control run.

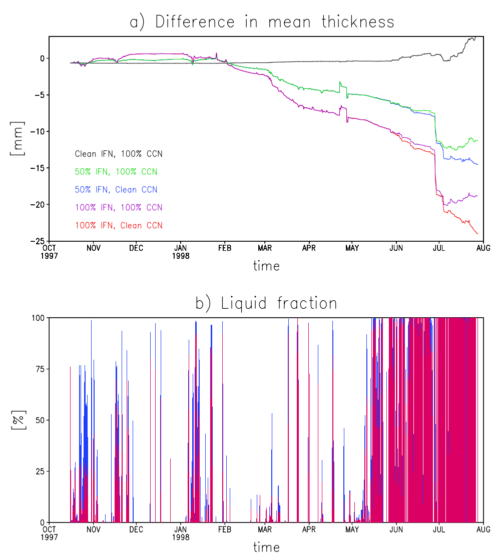

Figure 3. Ice thickness difference (a). Liquid water fraction for the control run (b). Blue indicates the control run while red, the run corresponding to the observed IFN and CCN concentrations.

Differences in Fig. 5a are negative for all experiments that consider enhanced IFN concentrations above the inversion, indicating larger melting rates (lower freezing rates) compared to the control case. Positive differences were obtained for the run that only takes into account CCN entrainment. Simulated mean sea-ice thickness decrease for upper layers more polluted in terms of IFN (assuming the same CCN profile). Conversely, the simulated thickness increase slightly when we enhance CCN (assuming the same IFN profile) only when liquid clouds prevail. The sign and the magnitude of these differences indicate that the CCN effect is opposite but less important than the IFN effect.

5. CONCLUSIONS

A series of multi-month CRM simulations have been performed covering both freezing and melting seasons. When assuming polluted initial profiles within the upper layer, the liquid water fraction of the cloud monotonically decreases, TCP increases, and LWDN tends to increase due to a significant increase in IWP. Results indicate that IFN entrainment of polluted air overriding the inversion may have a significant impact on sea-ice freezing/melting rates when mixed phase clouds are present, and CCN effect is opposite although less important. We must await daily observations of IFN and CCN profiles before we can determine the total impacts of aerosol intrusions into the Arctic on climate. However, the results suggested by these multi-month CRM simulations may have important climatological implications since the extent and duration of sea-ice coverage not only effects regional climate but also global climate through ice-albedo feedbacks.

6. ACKNOWLEDGEMENTS

This research was supported by a University of Alaska Fairbanks Research contract UAF-00-0086/FP100092 (CSU 5-33422) and by a NSF grant #0215367.

7. REFERENCES

Carrió, G.G., Jiang, H, and W. R. Cotton, 2003a: Impact of aerosol intrusions on Arctic boundary layer clouds Part I: May 4 1998 case. J. Atmos. Sci., conditionally accepted.

Carrió, G.G., Jiang, H, and W. R. Cotton, 2003b: Impact of aerosol intrusions on Arctic boundary layer clouds Part I: Sea-ice melting rates. J. Atmos. Sci., conditionally accepted.

Cotton,W. R., R.A. Pielke, Sr., R.L. Walko , G.E. Liston, C.J. Tremback, H. Jiang, R. L. McAnelly, J. Y. Harrington, M.E. Nicholls, G.G. Carrió and J. P. Mc Fadden 2003: RAMS 2001: Current Status and future directions. Meteor. Atmos. Physics, 82, 5-29.

Hunke, E. C., and Lipscomb, 1999: CICE: The Los Alamos se-ice model, documentation and software, version 2.0, Los Alamos National Laboratory,LA-CC-98-16, v.2.

Lipscomb, W. H, 2001: Remapping the Thickness Distribution of Sea-ice. J. Geophys. Res..Vol 106, 13989-14000.